

NASA CR-177,994

**NASA Contractor Report 177994**

**ICASE REPORT NO. 85-44**

NASA-CR-177994  
19860004751

---

# ICASE

A FOURTH-ORDER SCHEME FOR THE UNSTEADY  
COMPRESSIBLE NAVIER-STOKES EQUATIONS

Alvin Bayliss  
Paresh Parikh  
Lucio Maestrello  
Eli Turkel

RECEIVED  
DEC 23 1985

DEC 23 1985

LANGLEY RESEARCH CENTER  
LIBRARY, NASA  
HAMPTON, VIRGINIA

NASA Contracts No. NAS1-17070 and No. NAS1-17130  
October 1985

INSTITUTE FOR COMPUTER APPLICATIONS IN SCIENCE AND ENGINEERING  
NASA Langley Research Center, Hampton, Virginia 23665

Operated by the Universities Space Research Association

**NASA**  
National Aeronautics and  
Space Administration  
**Langley Research Center**  
Hampton, Virginia 23665



NF01019

**A FOURTH-ORDER SCHEME FOR THE  
UNSTEADY COMPRESSIBLE NAVIER-STOKES EQUATIONS**

A. Bayliss  
Exxon Corporate Research Science Laboratories

P. Parikh  
Vigyan Research Associates, Inc.

L. Maestrello  
NASA Langley Research Center

E. Turkel  
ICASE and Tel-Aviv University

**Abstract**

A computational scheme is described which is second-order accurate in time and fourth-order accurate in space (2-4). This method is applied to study the stability of compressible boundary layers. The laminar compressible Navier-Stokes equations are solved with a time harmonic inflow superimposed on the steady state solution. This results in spatially unstable modes. It is shown that the second-order methods are inefficient for calculating the growth rates and phases of the unstable modes. In contrast the fourth-order method yields accurate results on relatively course meshes.

---

Partial support was provided for the first author under NASA Contract No. NAS1-17070 and for the second author under NASA Contract No. NAS1-17252.

Research for the fourth author was supported by the National Aeronautics and Space Administration under NASA Contracts No. NAS1-17070 and NAS1-17130 while he was in residence at the Institute for Computer Applications in Science and Engineering, NASA Langley Research Center, Hampton, VA 23665.

## I. Introduction

This paper is concerned with a fourth-order accurate finite difference scheme for the compressible, unsteady Navier-Stokes equations. The primary interest is the computation of spatially unstable disturbances into the nonlinear regime and the active control of such disturbances. Due to the wavelike nature of these disturbances, this problem has features of both wave propagation and fluid dynamics and the numerical scheme must be chosen to accurately compute waves propagating in an unstable, high Reynolds number mean flow. The application of this scheme to study the active control of spatially growing disturbances has been described previously [1]. This paper describes the numerical scheme and the advantages that can be obtained by the use of fourth-order accuracy.

Higher order accurate methods, in particular spectral methods, have been successfully used in the computation of incompressible flows. Examples of such calculations can be found in [2] - [4]. Generally, spectral methods assume that problem is periodic in the streamwise direction so that Fourier (as opposed to Chebyshev) collocation can be used. (Spatially unstable disturbances were considered, however in [4].) The use of higher order methods for the numerical computation of waves has also been extensively considered in the literature. Examples can be found in [5] - [7].

In section 2, we describe the numerical scheme and discuss certain implementation details. In section 3 the performance of this scheme on a variety of problems is illustrated. Finally, in section 4 we discuss these results and draw conclusions.

## II. Numerical Scheme

The numerical scheme is an extension of the second-order MacCormack scheme due to Gottlieb and Turkel [8]. For the one-dimensional equation  $U_t = F_x$  where  $F = F(U)$ , we have (letting the superscripts denote the time level and the subscripts denote the spatial grid points)

$$\bar{U}_i = U_i^n + \frac{\Delta t}{6\Delta x} \left[ 7(F_{i+1}^n - F_i^n) - (F_{i+2}^n - F_{i+1}^n) \right] \quad (2.1a)$$

$$U_i^{n+1} = \frac{1}{2} \left\{ U_i^n + \bar{U}_i + \frac{\Delta t}{6\Delta x} \left[ 7(\bar{F}_i - \bar{F}_{i-1}) - (\bar{F}_{i-1} - \bar{F}_{i-2}) \right] \right\} \quad (2.1b)$$

There is an obvious symmetric variant of (2.1) starting with a backwards predictor and then a forwards corrector.

If  $F$  depends only on  $U$  it is shown in [8] that the scheme (2.1) is second-order accurate in time and fourth-order accurate in space ((2-4) scheme). Specifically, if  $\Delta t$  is the time step and  $\Delta x$  the space step, then the truncation error is  $O(\Delta t((\Delta x)^4 + (\Delta t)^2))$ . Thus the scheme is fourth-order accurate provided  $\Delta t = O((\Delta x)^2)$  as  $\Delta x \rightarrow 0$ . For nonlinear problems this is true only if the two variants of (2.1) are alternated.

Although true fourth-order accuracy is obtained only for  $\Delta t = O((\Delta x)^2)$  it has been found that (2.1) is considerably more efficient than second-order schemes (see for example [6], [9-10]). For two-dimensional problems (2.1) can be used together with operator splitting [11] to maintain the (2-4) accuracy. Specifically, for the equation

$$U_t = F_x + G_y$$

we have

$$U^{n+2} = L_x L_y L_y L_x U^n$$

where  $L_x$  and  $L_y$  are one-dimensional solution operators corresponding to the scheme (2.1) applied to the equations  $U_t = F_x$  and  $U_t = G_y$  respectively. Alternatively, one can consider an unsplit version of (2.1) [12].

The explicit nature of the scheme (2.1) makes it well suited for current vector computers such as the CDC Cyber 205 and the Cray 1-S and XMP series. The scheme has been implemented on the CDC VPS 32 at NASA Langley Research Center using vector operations over a two-dimensional grid (vector lengths  $\sim 20,000$ ). The explicit nature of the scheme makes it relatively inefficient to compute steady flow, unless acceleration techniques are incorporated [13]. For the unsteady flows considered here, a time step restriction is necessary in order to accurately resolve the fluctuations in time and so explicit schemes become efficient.

The implementation of the scheme (2.1) is straightforward if the flux function  $F$  depends only on the unknown  $U$ . For the Navier-Stokes equations we have  $F = F(U, U_x, U_y)$  and in the evaluation of  $F_i$  it is necessary to approximate  $U_x$  [8]. For a forward sweep, i.e., (2.1a)  $U_x$  is approximated by a two-point backwards difference, i.e.,  $U_x \sim U_i - U_{i-1}/\Delta x$  and conversely for a backwards sweep. It is shown in [8] that for a general, non-constant coefficient problem this results in a scheme that is only third-order accurate. However, it can be shown that the third-order truncation error is eliminated by alternating the sweeps and the resulting scheme is fourth-order accurate for both the inviscid and viscous terms. Mixed derivatives, i.e., terms of the form  $U_y$  in an  $x$  sweep are approximated by second-order central differences. In many applications these terms are relatively small. We have not experimented with fourth-order differences for these terms.

In order to complete the description of the numerical scheme, it is necessary to describe the implementation of boundary conditions. We distinguish between boundary conditions which must be imposed as part of the problem and those boundary conditions which are necessary because the straightforward application of the difference formula (2.1) is not valid at boundary points. In this section we consider only the latter.

Consider the forward predictor (2.1a). If  $i = N$  denotes a boundary point then the values of  $F_i$  are not available for  $i > N$  and thus the scheme (2.1) can not be applied at the points  $i = N-1$  and  $i = N$ . The most satisfactory boundary treatment that we have found is to define  $F_i$  for  $i > N$  by third-order extrapolation from the interior (see [6] and [8]). Hence,  $F_{N+1}$  and  $F_{N+2}$  are defined by

$$F_{N+1} = 4F_N - 6F_{N-1} + 4F_{N-2} - F_{N-3} \tag{2.2}$$

$$F_{N+2} = 4F_{N+1} - 6F_N + 4F_{N-1} - F_{N-2}.$$

In (2.2) the extrapolated fluxes include both the viscous and inviscid terms.

The scheme (2.1) has a five-point stencil. Implicit fourth-order schemes with a three-point stencil can be constructed by using Padé approximations. It is well known that compact schemes are more accurate than five-point schemes [14], however, they are more expensive because of the implicit nature of the scheme. One way to increase the accuracy of the scheme (2.1) is to use a scheme which is sixth-order accurate in space. The scheme (2.1) can be easily extended to sixth-order. The resulting scheme is

$$\bar{U}_1 = U_1^n + \frac{\Delta t}{30\Delta x} [37(F_{1+1}^n - F_1^n) - 8(F_{i+2}^n - F_{1+1}^n) + (F_{1+3}^n - F_{1+2}^n)] \quad (2.3a)$$

$$U_1^{n+1} = \frac{1}{2} \left\{ U_1^n + \bar{U}_1 + \frac{\Delta t}{30\Delta x} [37(\bar{F}_1 - \bar{F}_{i-1}) - 8(\bar{F}_{i-1} - \bar{F}_{1-2}) + (\bar{F}_{1-2} - \bar{F}_{1-3})] \right\}. \quad (2.3b)$$

The suitability of (2.3) for the unsteady Navier-Stokes equations is currently being investigated.

### III. Numerical Examples

In this section we describe some numerical examples illustrating the effects that can be expected from the fourth-order accurate differencing. The present program is primarily designed to compute unsteady flows and does not make use of any acceleration techniques which destroy the consistency in time [13]. The first numerical example will, however, illustrate the effect of the higher-order differencing on steady flows.

Specifically, we consider a supersonic boundary layer over a flat plate. The free stream Mach number is 4.5 and the unit Reynolds number is  $2.3 \times 10^6$ . The inflow data is generated by a boundary layer program [15] at 0.5 ft. from the leading edge. The computational domain is 2.0 ft. in  $x$  and  $11 \delta$  in  $y$  where  $\delta$  is the boundary thickness at inflow. An exponentially stretched grid is used normal to the plate with the Jacobians evaluated analytically. Figure 1 illustrates the computational domain.

In addition to the numerical boundary treatment described previously, it is necessary to discuss the boundary conditions which must be imposed. For

the supersonic case all quantities are imposed at the inflow while the solution at the outflow boundary is obtained by zeroth-order extrapolation from the interior. We have verified that the solution is very insensitive to the treatment of the outflow boundary as would be expected since the linearized characteristic variables are convected out of the computational domain. At the plate, the two velocity components are set to zero and the temperature is specified. Several different techniques have been used to obtain the pressure. These include different orders of extrapolation in the normal direction and the use of the normal momentum equation. The accuracy of the solution is insensitive to the boundary treatment (probably because of the stretched grid). At present we simply use first-order extrapolation for the pressure.

The treatment of the upper boundary (see Fig. 1) is based on the linearized characteristics in the normal direction.

The Navier-Stokes equations can be written in the generic form

$$U_t = F_x + G_y \quad (3.1)$$

where  $U$  is the vector  $(\rho, \rho u, \rho v, E)^T$ ,  $\rho$  is the density,  $u$  and  $v$  are the  $x$  and  $y$  velocities, respectively and  $E$  is the total energy. The functional forms of  $F$  and  $G$  are standard and are omitted for brevity. In the normal direction we consider only the system

$$U_t = G_y. \quad (3.2)$$

In the applications the vertical velocity  $v$  is small and positive at the upper boundary. Upon linearizing (3.2) we find that the three characteristic

variables

$$p - \rho \tilde{c}^2 \quad (3.3a)$$

$$p + \rho \tilde{c} v \quad (3.3b)$$

$$u \quad (3.3c)$$

are convected to the boundary from the interior. These three variables are obtained by zeroth-order extrapolation from the interior. Since we consider the linearized characteristics, the quantities with a  $\tilde{\sim}$  in (3.3), are taken from the previous time step. The final boundary condition is obtained from setting

$$p_t - \rho \tilde{c} v_t = 0 \quad (3.3d)$$

corresponding to the characteristic variable entering the computational region. The use of the radiation condition (3.3d) was previously found to considerably accelerate the convergence to the steady state and to permit the upper boundary to be brought closer to the plate [16].

A typical comparison between the second and fourth-order schemes is shown in Fig. 2. The streamwise velocity is plotted against  $y$  at a location of 1.0 ft. from the leading edge ( $Re_{\delta^*} = 17174$ ), where  $Re_{\delta^*}$  is the Reynolds number based on displacement thickness. The results are shown for the fourth-order scheme (2.1), the second-order MacCormack scheme and the solution obtained from the boundary layer equations. The finite difference results were obtained from the same grid ( $21 \times 31$ ) and the improvement in accuracy of the fourth-order scheme is evident. It should be noted that we do not obtain a similar improvement for more viscous boundary layers. The reason for this is not understood and is currently being investigated.

For our next example, we consider an unsteady disturbance in a relatively low speed subsonic boundary layer. The mean flow is a boundary layer with free stream Mach number 0.4 and a unit Reynolds number of  $3.0 \times 10^5$ . At inflow we have  $Re_{\delta}^* = 998$  and the computational domain is chosen so that at outflow  $Re_{\delta}^* = 1730$ . A fluctuating disturbance is introduced at the inflow with nondimensional frequency  $F = (2\pi f\nu)/U_{\infty}^2$  of  $.8 \times 10^4$ .  $f$  is the frequency in Hertz,  $\nu$  the kinematic viscosity, and  $U_{\infty}$  the free stream velocity. This flow is nearly incompressible. Based on linear, incompressible stability theory it is known that this frequency is unstable at inflow but becomes stable at  $Re_{\delta}^* = 1450$ . Since this is a subsonic flow, three boundary conditions must be imposed at the inflow. These conditions are obtained by computing an eigenfunction of the Orr-Sommerfeld equations (using a program developed by R. Dagenhart of NASA Langley Research Center). The real part of the solution (times  $e^{iFt}$ ), is then used to compute the three linearized characteristic variables which enter the computational domain from the outside. Specifically,

$$\left. \begin{array}{l} p + \tilde{\rho}c\tilde{u} \\ p - \tilde{\rho}c^2 \\ v \end{array} \right\} = \text{mean} + \epsilon \text{ (values obtained from Orr-Sommerfeld equation)} \quad (3.4a)$$

where  $\epsilon$  determines the strength of the disturbance. The outgoing characteristic variable  $p - \tilde{\rho}c\tilde{v}$  is obtained from the interior by zeroth-order extrapolation.

The outflow boundary condition is treated similarly. The incoming characteristic variable is set equal to zero by imposing the condition

$$p_t - \tilde{\rho} \tilde{c} u_t = 0. \quad (3.5)$$

The use of the condition (3.5) and more accurate radiation condition to compute unsteady disturbances in subsonic flows is discussed in [16]. Characteristic radiation boundary conditions of the form (3.5) are commonly used in two-dimensional linear wave propagation problems (for example, see [17]). The boundary condition (3.5) has been found to be sufficiently accurate for the present calculations. This is based on comparisons with linear stability theory.

In Fig. 3 we plot the computed growth rate as a function of  $Re_{\delta}^*$ . The growth rates are computed by calculating the  $RMS = \sqrt{\overline{(\rho u)^2} - \overline{(\rho u)_{mean}^2}}$  and integrating in  $y$ . The inflow data is chosen so that the maximum perturbation is 2% of the free stream. In this case the (2-4) scheme shows a significant amount of nonlinear growth while the (2-2) scheme, for the same grid, shows significantly less growth. Mesh refinements verify the accuracy of the fourth-order code.

Reducing the inflow perturbation to 0.2% of the free stream the fourth-order results reproduce the linear theory results very closely and in particular, show that the perturbation becomes stable at  $Re_{\delta}^* \sim 1450$  as predicted by linear theory.

In Figs. 4a and 4b we plot  $\rho u$  as a function of time for  $Re_{\delta}^* = 1263$  and  $y = 0.0034$  ft. In Fig. 4a the (2-4) scheme is shown for two different grids and shows that a further grid refinement does not yield any additional information. In Fig. 4b the (2-2) scheme is compared with the (2-4) scheme. At this location the disturbance is basically linear and the figures indicate significant amplitude and phase errors for the (2-2) scheme.

Figures 5a and 5b contain similar results further downstream at the location  $Re_{\delta}^* = 1481$  and  $y = 0.0011$  ft. At this location the disturbance exhibits some nonlinear effects which are not found by the second-order scheme with this mesh.

In Fig. 6 the computed growth rates are shown for a disturbance in higher speed flow where compressibility effects would be expected to be important. The free stream Mach number is 0.7 and the unit Reynolds number is 300,000. The computational domain is chosen so that at inflow we have  $Re_{\delta}^* = 900$ . The nondimensional frequency  $F = 0.8 \times 10^4$ . The inflow data was generated from the incompressible stability program, however, we have not compared growth rates with those predicted by the incompressible stability theory. The results in Fig. 6 show a significant reduction in the growth rate using the second-order scheme. Finally, in Fig. 7 we plot the mean of  $\rho u$  across the boundary layer for  $Re_{\delta}^* = 1400$ . It is apparent that the second-order scheme misses significant features of the flow.

## V. Conclusion

There are several types of errors that appear in the computation of unsteady waves and stability analysis. These include both amplitude and phase errors. These errors frequently simulate an apparent lower Reynolds number and indicate that the flow is more stable than it physically is. These effects are seen in the results presented here. It is shown that second-order, in space, schemes are not efficient in simulating nonlinear stability of high Reynolds number flows. The existing program solves the two-dimensional laminar compressible Navier-Stokes equations and is currently being extended

to three dimensions. Both subsonic and transonic stability regions can be calculated using the improved fourth-order method.

### References

- [1] Bayliss, A., Maestrello, L., Parikh, P., and Turkel, E., "Numerical Simulation of Boundary Layer Excitation by Surface Heating/Cooling," AIAA Paper 85-0565, March 1985.
- [2] Malik, M., Zang, T. A., and Hussaini, M. Y., "A Spectral Collocation Method for Navier-Stokes Equations, ICASE Report 84-19, NASA CR-172365, June 1984.
- [3] Orszag, S. A. and Kells, L. C., "Transition to Turbulence for Plain Poiseuille Flow and Plain Couette Flow," J. Fluid. Mech., Vol. 96, 1980, pp. 159-205.
- [4] Murdock, J. W., "A Numerical Study of Nonlinear Effects on Boundary Layer Stability," AIAA J., Vol. 15, No. 8, 1977, pp. 1167-1173.
- [5] Kreiss, H. O. and Olinger, J., "Comparison of Accurate Methods for the Integration of Hyperbolic Systems," Tellus, Vol. 24, 1972, pp. 119-225.
- [6] Turkel, E., "On the Practical Use of Higher-Order Methods for Hyperbolic Systems," J. Comput. Phys., Vol. 35, 1980, pp. 319-340.
- [7] Alford, R. M., Kelly, K. R., and Borre, D. M., "Accuracy of Finite Difference Modeling of the Acoustic Wave Equation," Geophysics, Vol. 39, No. 6, 1974, pp. 834-842.

- [8] Gottlieb, D. and Turkel, E., "Dissipative Two-Four Methods for Time Dependent Problems," Math. Comp., Vol. 30, 1976, pp. 703-723.
  
- [9] Maestrello, L., Bayliss, A., and Turkel, E., "On the Interaction between a Sound Pulse with the Shear Layer of an Axisymmetric Jet," J. Sound and Vib., Vol. 74, No. 2, January 1981, pp. 281-301.
  
- [10] Hariharan, S. I. and Lester, H. C., "Acoustic Shocks in a Variable Area Duct Containing Near Sonic Flows," J. Comput. Phys., Vol. 58, 1985, pp. 134-145.
  
- [11] Strang, W. G., "On the Construction and Comparison of Difference Schemes," SIAM J. Numer. Anal., Vol. 5, 1968, pp. 506-517.
  
- [12] Rudy, D. H., "Navier-Stokes Solutions for Two-Dimensional Subsonic Base Flow," Southeastern Conference on Theoretical and Applied Mechanics, May 1984.
  
- [13] Turkel, E., "Acceleration to a Steady State for the Euler Equation," ICASE Report 84-32, NASA CR-172398, July 1984.
  
- [14] Swartz, B and Wendroff, B., "The Relative Efficiency of Finite Difference and Finite Element Methods: I. Hyperbolic Problems and Splines," SIAM J. Numer. Anal., Vol. 11, 1974, pp. 979-993.

- [15] Harris, J. E. and Blanchard, D. K., "Computer Program for Solving Laminar, Transitional or Turbulent Compressible Boundary Layer Equations for Two-Dimensional and Axisymmetric Flow," NASA TM 83207, 1985.
  
- [16] Bayliss, A. and Turkel, E., "Far Field Boundary Conditions for Compressible Flows," J. Comput. Phys., Vol. 48, 1982, pp. 182-199.
  
- [17] Cohen, M. F., et al., "A Comparison of Paraxial and Viscous Silent Boundary Methods in Finite Element Analysis," Joint ASME-ASCE Mechanics Conference, University of Colorado, 1981, pp. 67-80.

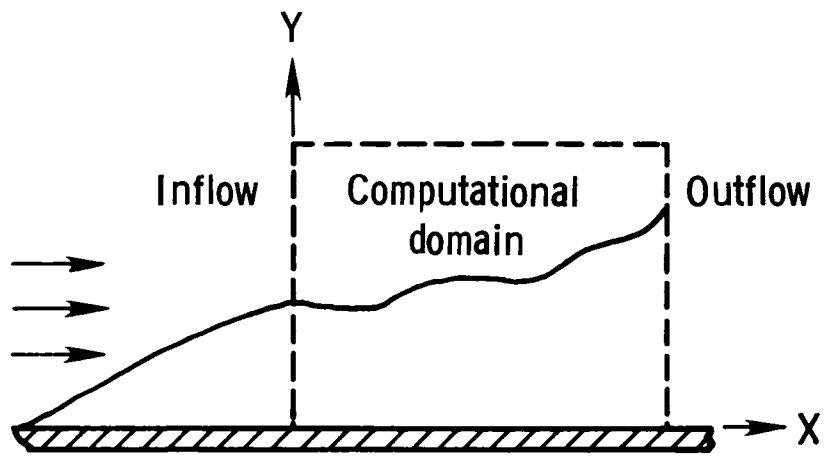


Fig. 1. Schematic of computational domain.

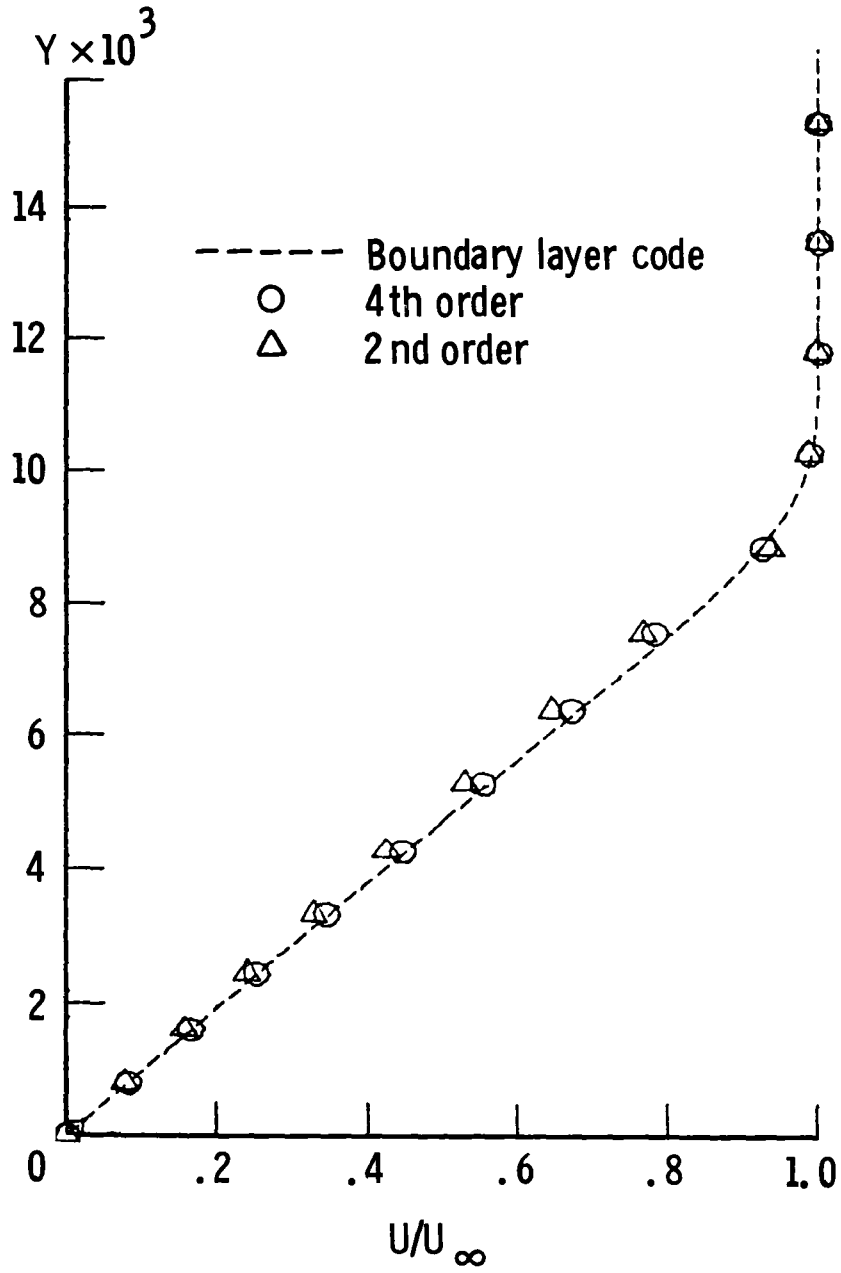


Fig. 2. Comparison between the second and the fourth-order schemes for a steady state.  $M_{\infty} = 4.5$ .

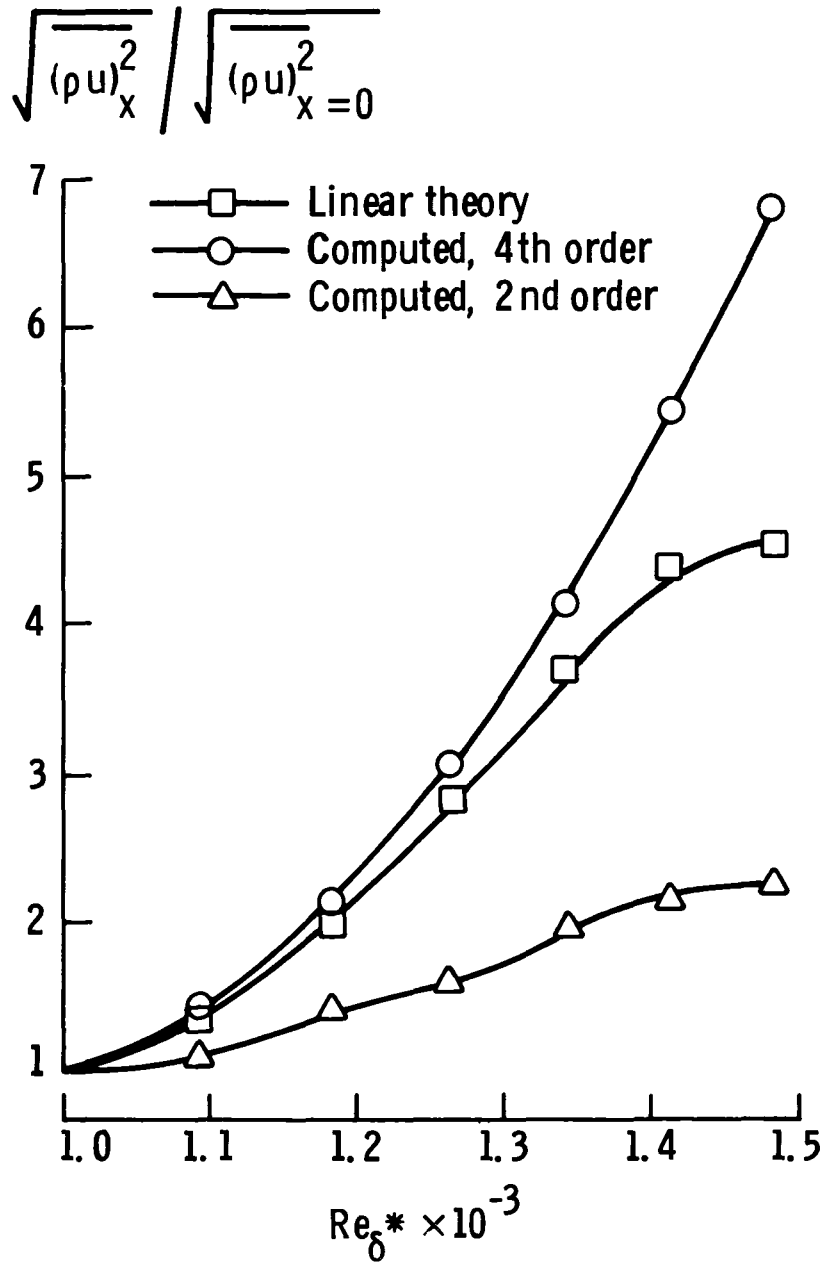


Fig. 3. Comparison of amplitude growth for the second and the fourth-order schemes.  $M_\infty = 0.4$ .

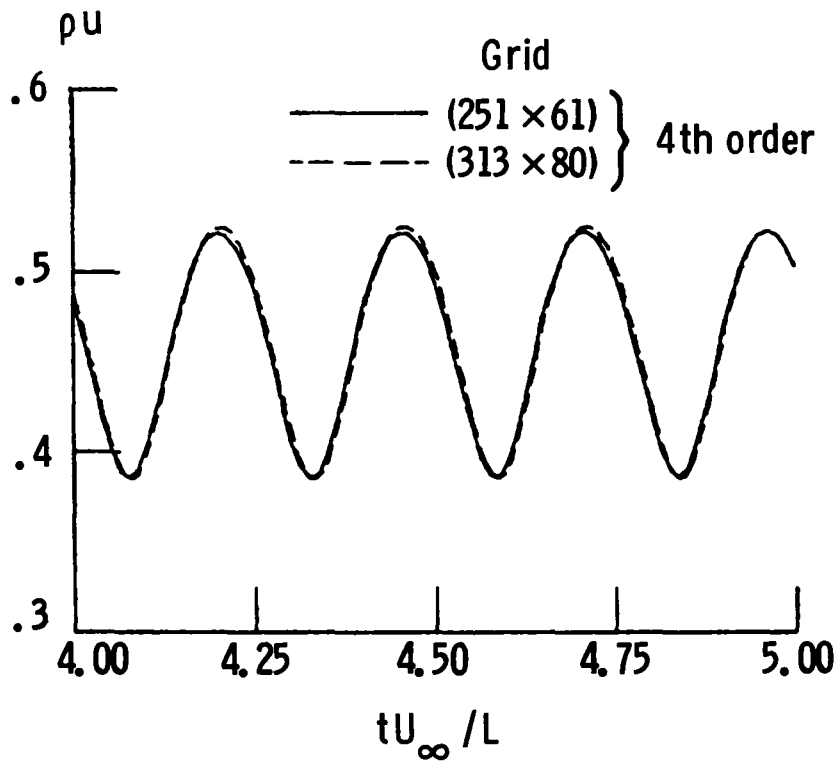


Fig. 4a.  $\rho u$  vs. time for two grids at  $Re_\delta^* = 1263$ ,  $y = 0.0034$  ft.

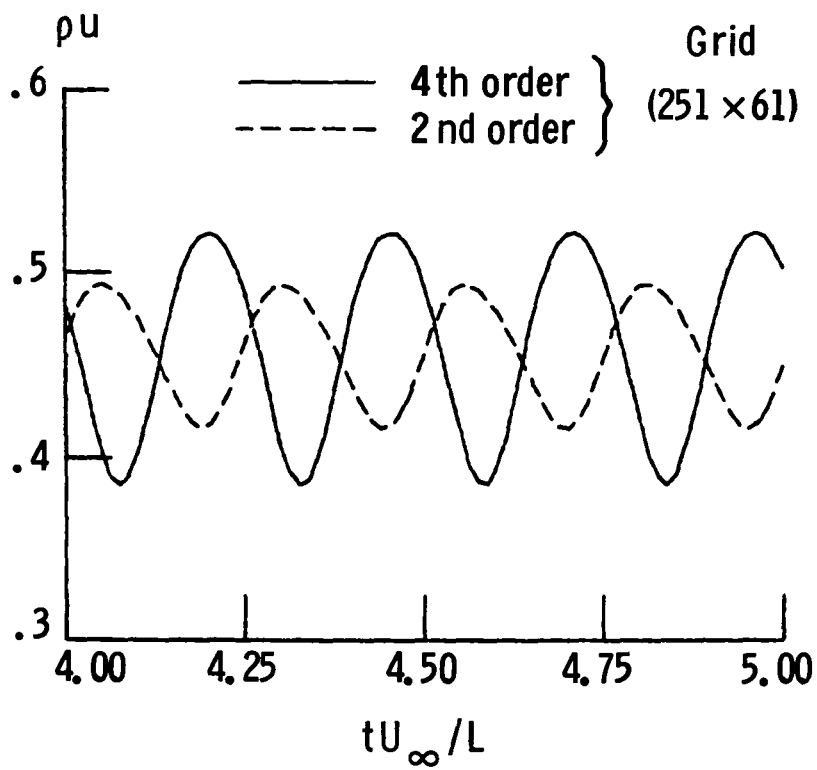


Fig. 4b.  $\rho u$  vs. time using second and fourth-order schemes.

$$Re_{\delta^*} = 1263, y = 0.0034 \text{ ft.}$$

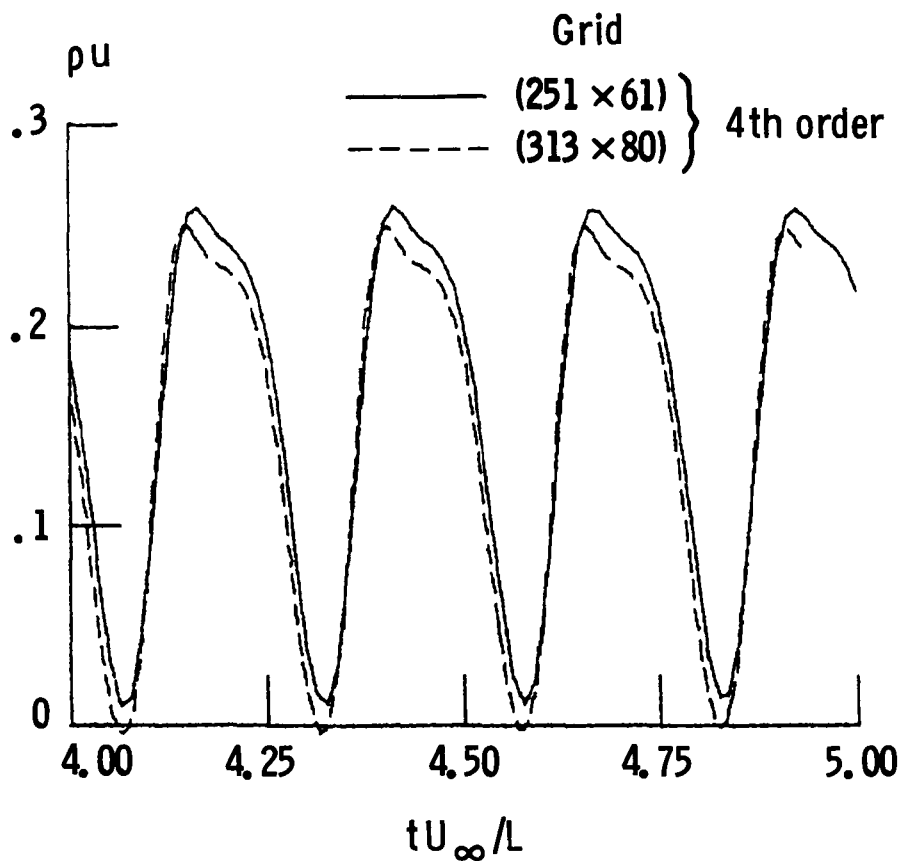


Fig. 5a. pu vs. time for two grids at  $Re_{\delta^*} = 1481$ ,  $y = 0.0011$  ft.

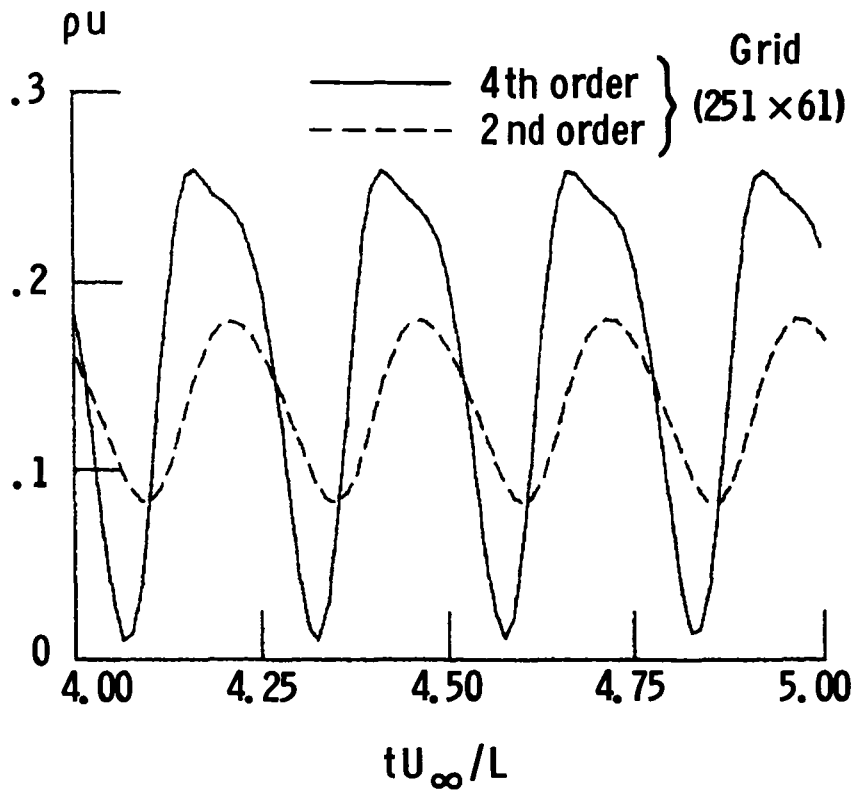


Fig. 5b.  $\rho u$  vs. time using second and fourth-order schemes.

$$Re_{\delta^*} = 1481, \quad y = 0.0011 \text{ ft.}$$

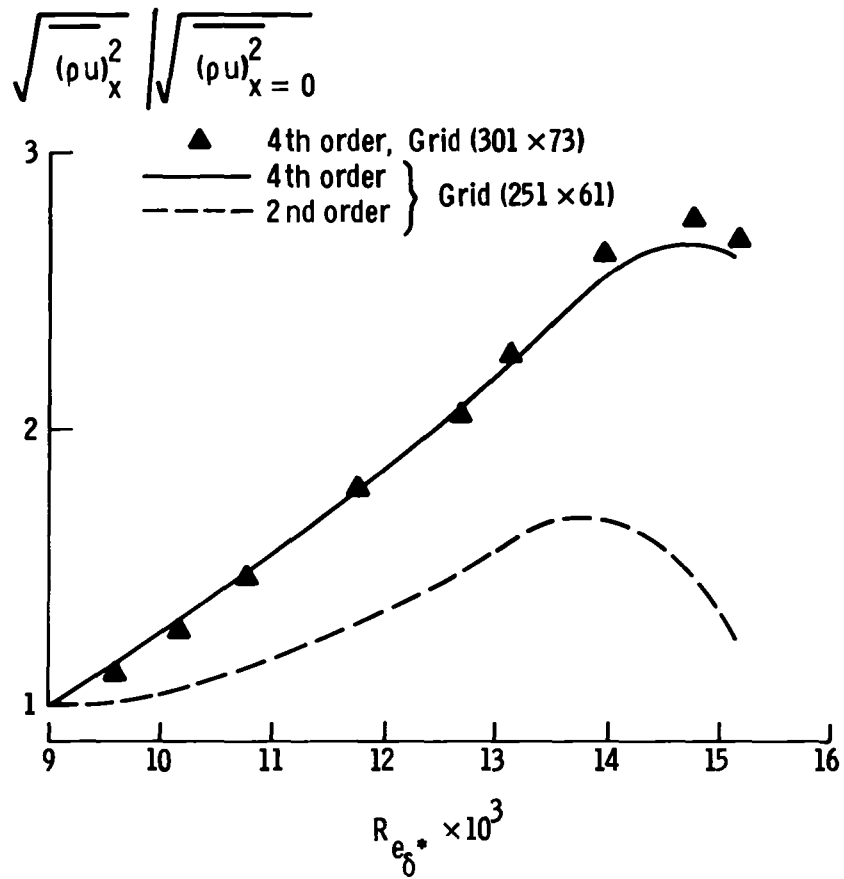


Fig. 6. Comparison of amplitude growth for the second and the fourth-order schemes.  $M_\infty = 0.7$ .

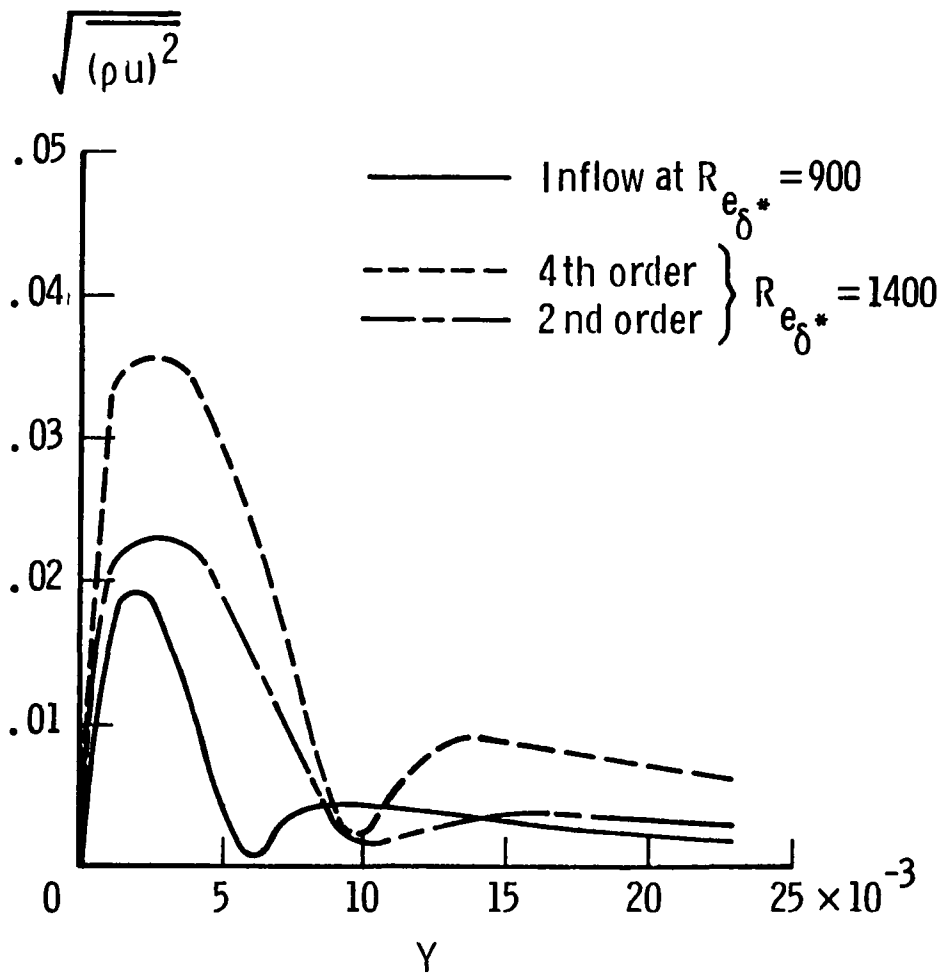


Fig. 7. RMS amplitude distribution across the boundary layer.

1 Report No NASA CR-177994 ICASE Report No. 85-44		2 Government Accession No		3 Recipient's Catalog No	
4 Title and Subtitle A FOURTH-ORDER SCHEME FOR THE UNSTEADY COMPRESSIBLE NAVIER-STOKES EQUATIONS				5 Report Date October 1985	
				6 Performing Organization Code	
7 Author(s) A. Bayliss, P. Parikh, L. Maestrello, and E. Turkel				8 Performing Organization Report No 85-44	
				10 Work Unit No	
9 Performing Organization Name and Address Institute for Computer Applications in Science and Engineering Mail Stop 132C, NASA Langley Research Center Hampton, VA 23665				11 Contract or Grant No NAS1-17070; NAS1-17130	
				13 Type of Report and Period Covered <u>Contractor Report</u>	
12 Sponsoring Agency Name and Address National Aeronautics and Space Administration Washington, D.C. 20546				14 Sponsoring Agency Code 505-31-83-01	
15 Supplementary Notes Langley Technical Monitor: J. C. South Jr. <span style="float: right;">Submitted to AIAA J.</span> Final Report					
16 Abstract  A computational scheme is described which is second-order accurate in time and fourth-order accurate in space (2-4). This method is applied to study the stability of compressible boundary layers. The laminar compressible Navier-Stokes equations are solved with a time harmonic inflow superimposed on the steady state solution. This results in spatially unstable modes. It is shown that the second-order methods are inefficient for calculating the growth rates and phases of the unstable modes. In contrast the fourth-order method yields accurate results on relatively course meshes.					
17 Key Words (Suggested by Author(s)) fourth-order, stability, boundary layer, Navier-Stokes equations			18 Distribution Statement 02 - Aerodynamics 34 - Fluid Mech. and Heat Transfer  Unclassified - Unlimited		
19 Security Classif (of this report) Unclassified	20 Security Classif (of this page) Unclassified	21 No of Pages 25	22 Price A02		

**End of Document**